

Cobalt-57 and Technetium-99m-HMPAO-Labeled Leukocytes for Visualization of Ischemic Infarcts

Henk Stevens, Christoph Van de Wiele, Patrick Santens, Hugo M.L. Jansen, Jacques De Reuck, Rudy Dierckx and Jakob Korf
Departments of Nuclear Medicine and Neurology, University Hospital Ghent, Ghent, Belgium; and Department of Biological Psychiatry, University Hospital Groningen, Groningen, the Netherlands

Previous studies have shown the usefulness of divalent cobalt isotopes to visualize cerebral damage after stroke. The site of accumulation of cobalt ion is unknown but may be explained by neuronal influx, analogous to that of calcium ion. Additionally, uptake may be due to infiltrating leukocytes or protein-bound cobalt. The aims of this study were to compare ^{57}Co -SPECT with leukocyte SPECT and to compare the SPECT findings with clinical outcome as scored by the Orgogozo scale. **Materials:** Ten patients with a CT scan positive for middle cerebral artery infarcts were included in the study (7 men, 3 women; mean age 70 yr). Technetium-99m leukocyte and cobalt-SPECT (interval 2–4 days) were made with a double-headed gamma camera, after the injection of 10–15 mCi $^{99\text{m}}\text{Tc}$ -HMPAO-labeled leukocytes and 0.4 mCi ^{57}Co , respectively. Scans were performed within 5–30 days after onset of the first symptoms. Regions of interest (ROI) containing the area of infarction in the slices displaying enhanced radioactivity or the middle cerebral artery (MCA) region in four successive slices were defined for calculating enhancement ratios. The $^{99\text{m}}\text{Tc}$ leukocyte enhancement ratio (LER) and cobalt enhancement ratio (CER) were defined as the quotient of radioactivity in the ROI and an identical contralateral ROI. The MCA stroke-scale according to Orgogozo was used to assess neurological deficits at the time of scanning and discharge. **Results:** Cobalt-57 and $^{99\text{m}}\text{Tc}$ -HMPAO showed uptake in the infarcted brain area in five patients; the quantitative uptake in the infarcted brain area of the two tracers correlated significantly ($p < 0.05$). Both the LER and the CER correlated significantly ($p < 0.05$) with the Orgogozo score at the time of scanning. Only the LER correlated significantly ($p < 0.05$) with the Orgogozo score at discharge. **Conclusion:** Uptake of cobalt and leukocytes in the peri-infarct tissue suggests that ^{57}Co may visualize a component of the inflammatory response. Divalent ^{57}Co may be convenient to predict clinical prognosis after stroke.

Key Words: cerebral ischemia; stroke; leukocyte; cobalt-57; SPECT; technetium-99m-HMPAO

J Nucl Med 1998; 39:495–498

Leukocyte infiltration into the ischemic brain tissue has been demonstrated in clinical SPECT studies (1–4) and in experimental stroke models (5,6). After stroke, leukocytes accumulate mainly in the hypoperfused rim surrounding the core of infarction. This postischemic influx of leukocytes is not only a pathophysiologic response to injury but may aggravate ischemic damage during reperfusion as well as by obstruction of capillaries, initiating thrombosis and by releasing cytotoxic products including free radicals (7–11). Calcium is thought to play an important role in both the necrotic damage of ischemic brain tissue and in inflammatory responses after stroke (12–16). Both in vivo and in vitro experiments have shown that calcium accumulates in the (ir)reversibly damaged nerve cell body and in degenerating axons (14,17–21). To visualize calcium-mediated

damage, the divalent cobalt isotopes, ^{55}Co in PET and ^{57}Co in SPECT, have been previously proposed. Several investigations have already shown the usefulness of these cobalt isotopes to visualize stroke, traumatic brain injury, brain tumors and multiple sclerosis (3,22–27). The cellular site of accumulation of radioactivity is, as yet, not known. Therefore, the aims of this study were to compare ^{57}Co -SPECT with leukocyte SPECT and to compare the severity and the time-course of the impairment after stroke as assessed with the Orgogozo scale (28) with either SPECT imaging method.

MATERIALS AND METHODS

Patients

Ten patients (7 men; 3 women; age 58–80 yr; mean age 70 yr) with a middle cerebral artery (MCA) territory-ischemic infarction admitted to the neurological department were selected for ^{57}Co and $^{99\text{m}}\text{Tc}$ -HMPAO-labeled leukocyte-SPECT study. This study was approved by the Medical Ethics Committee of the University Hospital of Ghent, Belgium, and was conducted according to the principles of Good Clinical Practice. Inclusion criteria were stable clinical signs of MCA-infarction, 18 yr or older and written informed consent. Site of infarction was confirmed by CT. Patients with a disabling previous stroke, serious other disorders or deterioration in the course of MCA-stroke were excluded. The 10 patients formed a homogeneous group with respect to the diagnosis of MCA-infarction but differed regarding the time-interval between stroke-onset and SPECT examinations (5–30 days). The MCA stroke-scale according to Orgogozo (28) was used to assess neurological deficits. This MCA-scale evaluates level of consciousness, verbal communication, eye movement, power in arm, hand, leg and foot, and facial paresis on a score ranging from 0 (death) to 100 (complete recovery). Scoring was performed on day of scanning and discharge (at least 60 days after stroke-onset), when patients were clinically stable, and had demonstrated no further improvement for at least 14 days.

Technetium-99m-HMPAO-Labeled Leukocyte and Cobalt-57-SPECT

Autologous leukocytes were isolated and labeled with $^{99\text{m}}\text{Tc}$ -HMPAO (Ceretek[®], Amersham, Rainham, United Kingdom) using a previously described method (29). For incubation, a dose of 10–15 mCi $^{99\text{m}}\text{Tc}$ -HMPAO was used. Four hours following the injection of $^{99\text{m}}\text{Tc}$ -HMPAO-labeled leukocytes, SPECT was performed using a double-headed gamma camera (Elscint, Haifa, Israel) equipped with low-energy, high-resolution collimators. Data were acquired in a 128×128 matrix through a 360° rotation at an angular interval of 6° . Frame time was 30 sec. Filtering was performed using a Butterworth filter with a cutoff frequency of $0.50 f_{\text{Ny}}$, 13 order. Subsequently, images were re-oriented in the orbitomeatal plane, using externally applied point sources. Oblique, coronal and sagittal slices were obtained in each study. In each of the three planes, 16 images were obtained; 1–3 days later, 0.4 mCi $^{57}\text{CoCl}_2$ (Amersham, Rainham, United Kingdom) was

Received Feb. 3, 1997; revision accepted Apr. 23, 1997.

For correspondence or reprints contact: Jakob Korf, PhD, Department of Biological Psychiatry/Neuro PET Coordination, University Hospital Groningen, P.O. Box 30.001, 9700 RB Groningen, the Netherlands.

TABLE 1

Patient Characteristics, Orgogozo Scores and the Technetium-99m-HMPAQ-labeled Leukocyte SPECT and Cobalt-SPECT Data

Patient no.	Age (yr)	Sex	Interval (days)	ost ₁	ost ₂	ost ₁ -ost ₂	CER	LER
1	68	M	30	100	100	0	0.96	0.70
2	71	M	19	45	90	45	0.92	1.05
3	70	F	20	30	40	10	1.58	2.07
4	80	F	14	25	25	0	2.60	2.00
5	75	M	30	80	65	-15	0.92	1.03
6	64	M	11	45	85	40	1.60	1.80
7	65	F	9	75	80	5	1.04	0.93
8	64	M	15	70	90	20	1.05	0.84
9	59	M	15	70	85	15	1.10	1.37
10	74	M	5	45	45	0	1.78	5.25

Interval = time between onset of infarction and acquisition of ^{99m}Tc-HMPAQ-labeled leukocytes SPECT; ost₁ = neurological status as measured by MCA-scale (0-100) at time of cobalt-SPECT scanning; ost₂ = neurological status as measured by a MCA-scale (0-100) on discharge; ost₁-ost₂ = clinical improvement defined as the (positive) difference between the MCA-score on day of scanning and discharge; CER = cobalt enhancement ratio (quotient of the mean average cobalt-uptake in arbitrary units in the infarction versus the nonaffected brain); LER = leukocyte enhancement ratio (quotient of the mean average leukocyte uptake in arbitrary units in the infarction versus the nonaffected brain).

administered intravenously, and 24 hr later, ⁵⁷Co-SPECT was performed using the same double-headed gamma camera equipped with high-resolution, low-energy collimators. Filtering was performed using a Butterworth filter with a cutoff frequency of 0.50 f_{Ny} 13 order. Reconstruction and re-orientation was performed in an identical way as for ^{99m}Tc-HMPAQ-labeled leukocyte SPECT.

Data Analysis

For each MCA-stroke patient, sequential oblique SPECT-slices that were located in a 8-cm thick brain section displaying the actual infarction were analyzed visually. In those patients showing positive ⁵⁷Co or ^{99m}Tc-HMPAQ-labeled leukocyte accumulation, a region of interest (ROI) outlining the infarction-area was defined in each slice according to the location on CT scan. For each ROI in the infarcted area, an identical contralateral ROI was defined (mirror-ROI). The average ⁵⁷Co and ^{99m}Tc-HMPAQ-labeled leukocyte uptake in all ROIs was assessed. Data were combined to obtain the area as well as the labeled-leukocyte and cobalt-content of each ROI. The ^{99m}Tc-HMPAQ-labeled leukocyte enhancement ratio (LER) and cobalt enhancement ratio (CER) were defined as the quotient of radioactivity in the ROI versus mirror-ROI. In the patients showing no visually depictable ⁵⁷Co and ^{99m}Tc-HMPAQ-labeled leukocytes accumulation, semicircular ROIs encompassing the right and left middle cerebral artery territory in four successive slices were drawn with a manual cursor. Subsequently, using the infarcted site as a reference, hypothetical LER and CER were determined, allowing estimation of the normal variation in right to left (or vice versa) asymmetry. The possible relation between CER or LER and the Orgogozo scores were statistically evaluated using the nonparametric Spearman's rank correlation. Multiple regression analysis was performed to evaluate the relation between the time interval of LER or CER, Orgogozo-score at the time of the SPECT studies and the time interval. Correlations were defined as significant when p < 0.05.

RESULTS

Five patients suffered from a minor neurologic deficit (Orgogozo > 70) and showed no enhanced cobalt-uptake (0.96 < CER < 1.05) or leukocyte infiltration (0.70 < LER < 1.03) in

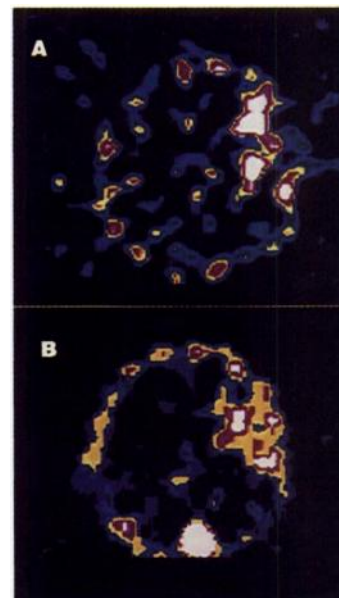


FIGURE 1. Brain SPECT scans of Patient 10, showing ⁵⁷Co (A) and ^{99m}Tc-HMPAQ-labeled leukocytes (B).

the affected MCA region. One patient suffered from cerebral ischemia with a large initial neurological deficit who revealed progressive improvement as shown by an increase in Orgogozo score and showed no enhanced cobalt-uptake (CER = 0.92) or leukocyte infiltration (LER = 1.05) in the affected MCA region. In the four patients presenting a major stroke (Orgogozo score 25-45) showing minor improvement, CER varied from 1.58-2.60 whereas the LER varied from 1.80-5.25. The uptake of the ⁵⁷Co and leukocytes tends to concur (Fig. 1). There was a significant correlation between CER and LER, as shown in Figure 2 (r = 0.65). The only notable exception was Patient 4, having a high accumulation of cobalt relative to that of the labeled leukocytes.

Analysis of the Orgogozo scores at time of scanning and discharge with the LER revealed for both a significantly negative correlation coefficient (r = - 0.8, p < 0.05, Fig. 3). Comparing CER and the Orgogozo scores at time of scanning and discharge showed only a significant negative correlation

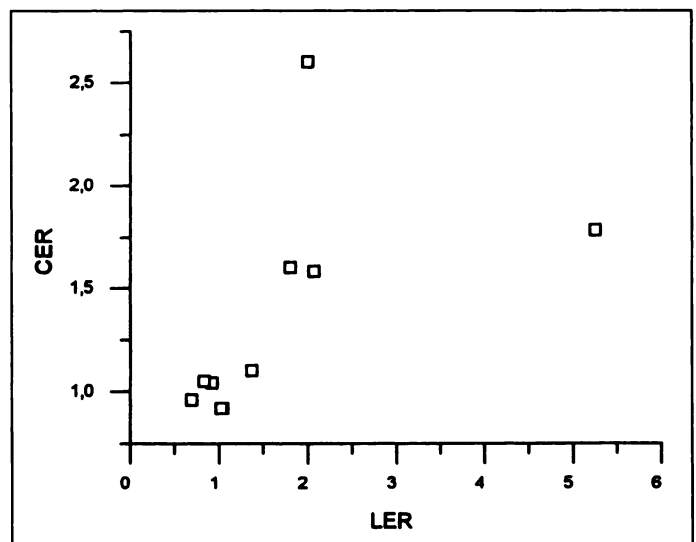


FIGURE 2. Relationship between uptake of leukocytes and cobalt in 10 stroke patients with mild-to-severe cerebral damage. The correlation coefficient between CER and LER was 0.74 (p < 0.05).

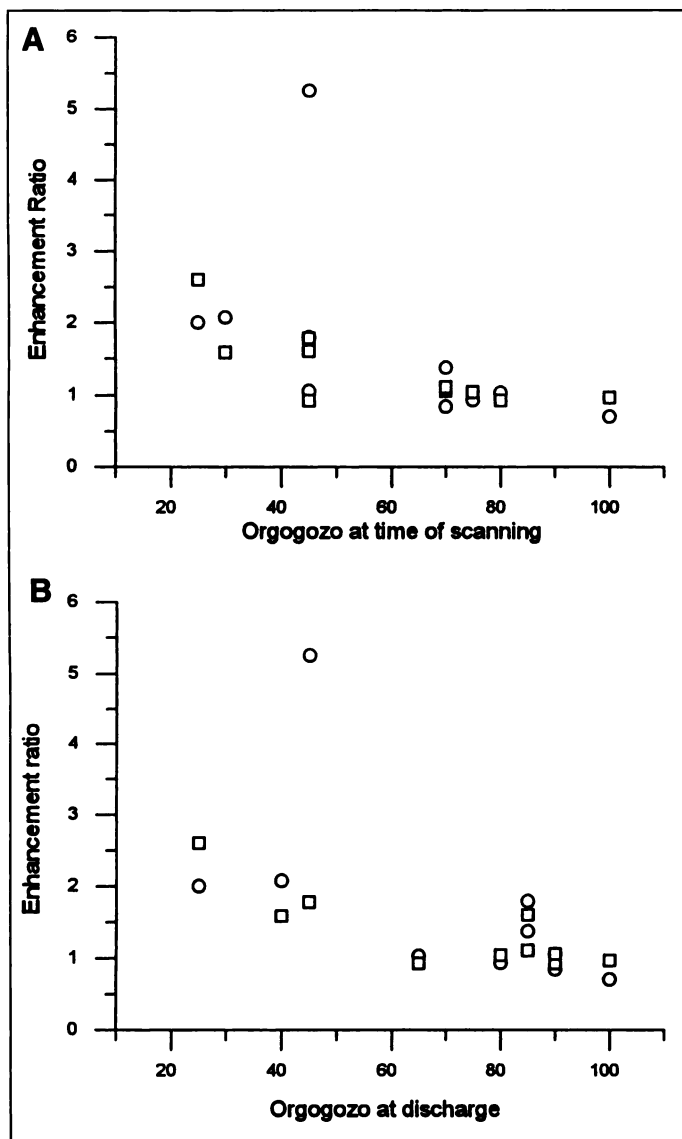


FIGURE 3. Relationship between the Orgogozo score at the time of scanning (ost_1) (A), discharge (ost_2) (B) and the relative uptake of lymphocytes (LER \circ) and ^{57}Co (CER \square). Analysis of the Orgogozo scores and enhancement ratios showed the following correlations: ost_1 -LER ($r = -0.8$, $p < 0.05$), ost_2 -LER ($r = -0.8$, $p < 0.05$), ost_1 -CER ($r = -0.7$, $p < 0.05$) and ost_2 -CER ($r = -0.6$, $p = 0.05$).

between Orgogozo score at time of scanning and CER ($r = -0.7$, $p < 0.05$, Fig. 3).

DISCUSSION

This study shows the concurrent accumulation of $^{57}\text{Co}^{2+}$ and $^{99\text{m}}\text{Tc}$ -HMPAO-labeled leukocytes in the ischemic area of cerebral infarcts. It is assumed that leukocytes often accumulate in the most severe infarcts (1-4), which is corroborated by the present results. The five patients without clear-cut accumulated radioactivity had only a slight neurological impairment, whereas the patients with the highest leukocyte infiltration suffered from a major stroke and showed little improvement. Our previous studies with ^{55}Co -PET showed that the radiotracer (presumably) accumulates in the perifocal tissue, surrounding the ischemic focus, which is the same tissue exhibiting inflammatory response and that is primarily infiltrated by leukocytes (22,23). The pattern of accumulation of $^{99\text{m}}\text{Tc}$ -HMPAO-labeled leukocytes was similar to that reported by Wang et al. (4) and others (1,2). These investigations showed that leukocyte infiltration is a dynamic process that persists for 5 wk and then

declines. The wide variance in LER (0.70-5.25) seen in our study (with 10 patients) is mainly due to the dynamic process of leukocytes accumulation. Since most leukocyte infiltration is found in the first week after a stroke, a high level of LER will also be found in the same time window. The uptake of both isotopes correlated with the actual neurological state as established by Orgogozo score, indicating to visualize neuronal damage reflecting functional impairment. Only LER correlated with the Orgogozo score at the time of discharge suggesting that leukocyte accumulation may not favor clinical improvement.

Cobalt was initially proposed to reflect calcium-influx in ischemically or neurotoxically affected nerve tissue (17,19,21,22). The cerebral uptake of intravenously administered radioactive calcium and cobalt shows high similarities in their localization in damaged tissue (17). It has become clear that the observed radioactivity cannot entirely be attributed to the diffusion of the free cations but also for at least a part to protein-bound calcium (and perhaps cobalt) (18,20). If this is also the case in this study, then cobalt-SPECT visualizes the opening of the blood-brain barrier towards serum proteins, including albumin. In *in vitro* experiments, the neuroprotective capacity of serum in glutamate-intoxicated neurons has been shown (30). If such a mechanism may also occur *in vivo*, then cobalt-SPECT or cobalt-PET may provide information about severity of the infarct and the protective potential in stroke.

In addition, the concurring uptake of cobalt and leukocytes in the peri-infarct tissue may indicate that ^{57}Co (and ^{55}Co) enables the visualization of inflammatory responses or processes concomitant with such responses. Since activation of leukocytes is accompanied by calcium uptake, the accumulation of exogenous calcium in ischemic brain tissue may also be attributed to infiltrating leukocytes. Considering the rather low radiation burden (25), its long half-life (270 days) and its inexpensive and simple preparation, ^{57}Co can be considered as a suitable isotope for establishing inflammatory response and clinical prognosis after stroke. The clinical value of cobalt-SPECT and cobalt-PET has to be assessed by comparison with other recent developed imaging tools in stroke (3,29,31,32).

CONCLUSION

Both $^{99\text{m}}\text{Tc}$ -HMPAO-labeled leukocyte and ^{57}Co SPECT visualize a pathophysiologic response in postischemic brain tissue characterized by a inflammatory reaction and changes that are associated with unfavorable clinical prognosis. Since the results of both imaging techniques concur, $^{99\text{m}}\text{Tc}$ -HMPAO leukocyte labeling procedure is labor intensive and the radiation burden associated with ^{57}Co is low (5 mSv), ^{57}Co should be considered as an alternative clinical imaging agent for this application.

ACKNOWLEDGMENTS

This work was supported by grant GGN 22.2741 from the Dutch Technology Foundation (STW) and grant 92.305 from the Netherlands Heart Foundation.

REFERENCES

- Kochanek PM, Hallenbeck JM. Polymorphonuclear leukocytes and monocytes/macrophages in the pathogenesis of cerebral ischemia and stroke. *Stroke* 1992;23:1367-1379.
- Silvestrini M, Pietroiusti A, Magrini A, et al. Leukocyte aggregation in patients with a previous cerebral ischemic event. *Stroke* 1994;25:1390-1392.
- Stevens H, Jansen HML, DeReuck J, Korf J. Imaging of stroke. In: Ter Horst GJ, Korf J, eds. *Clinical pharmacology of cerebral ischemia*. Totowa, NJ: Humana Press; 1997:31-42.
- Wang P-Y, Kao C-H, Mui, M-Y, Wang S-J. Leukocyte infiltration in acute hemispheric ischemic stroke. *Stroke* 1993;24:236-240.
- Jander S, Kraemer M, Schroeter M, Witte OW, Stoll G. Lymphocytic infiltration and expression of intercellular adhesion molecule-1 in photochemically induced ischemia of the rat cortex. *J Cereb Blood Flow Metab* 1995;15:42-51.

6. Nishino H, Czurko A, Fukuda A, et al. Pathophysiological process after transient ischemia of the middle cerebral artery in the rat. *Brain Res Bull* 1994;35:51-56.
7. Bowes MP, Rothlein R, Fagan SC, Zivin JA. Monoclonal antibodies preventing leukocyte activation reduce experimental neurologic injury and enhance efficacy of thrombolytic therapy. *Neurology* 1995;45:815-819.
8. Fassbender K, Mössner R, Motsch L, Kischka U, Grau A, Hennerici M. Circulating selectin- and immunoglobulin-type adhesion molecules in acute ischemic stroke. *Stroke* 1995;26:1361-1364.
9. Lefer DJ, Shandelya SML, Serrano CV, Becker LC, Kuppusamy P, Zweier JL. Cardioprotective actions of a monoclonal antibody against CD-18 in myocardial ischemia-reperfusion injury. *Circulation* 1993;88:1779-1787.
10. Wise RJ, Bernardi S, Frackowiak RS, Legg NJ, Jones T. Serial observations on the pathophysiology of acute stroke. The transition from ischaemia to infarction as reflected in regional oxygen extraction. *Brain* 1983;106:197-222.
11. Zhang RL, Chopp M, Li Y, et al. Anti-ICAM-1 antibody reduces ischemic cell damage after transient middle cerebral artery occlusion in the rat. *Neurology* 1994;44:1747-1751.
12. Araki T, Kato H, Inoue T, Kogure K. Long-term observations on calcium accumulation in postischemic gerbil brain. *Acta Neurol Scand* 1991;83:244-249.
13. Dienel GA. Regional accumulation of calcium in postischemic rat brain. *J Neurochem* 1984;43:913-925.
14. Gramsbergen JB, van den Berg KJ. Regional and temporal profiles of calcium accumulation and glial fibrillary acidic protein levels in rat brain after systemic injection of kainic acid. *Brain Res* 1994;667:216-228.
15. Shirohani T, Shima K, Iwata M, Kita H, Chigasaki H. Calcium accumulation following middle cerebral artery occlusion in stroke-prone spontaneously hypertensive rats. *J Cereb Blood Flow Metab* 1994;14:831-836.
16. Siesjo BK, Bengtsson F. Calcium fluxes, calcium antagonists, and calcium-related pathology in brain ischemia, hypoglycemia, and spreading depression: a unifying hypothesis. *J Cereb Blood Flow Metab* 1989;9:127-140.
17. Gramsbergen JBP, Veenma-van der Duin L, Loopuijt L, Paans AMJ, Vaalburg W, Korf J. Imaging of the degeneration of neurons and their processes in rat or cat brain by $^{45}\text{CaCl}_2$ autoradiography or $^{55}\text{CoCl}_2$ positron emission tomography. *J Neurochem* 1988;50:1798-1807.
18. Linde R, Laursen H, Hansen AJ. Is calcium accumulation post-injury an indicator of cell damage? *Acta Neurochir* 1995;(suppl):66:15-20.
19. Nagy I, Pabla R, Matesz C, Dray A, Woolf CJ, Urban L. Cobalt uptake enables identification of capsaicin- and bradykinin-sensitive subpopulations of rat dorsal root ganglion cells in vitro. *Neuroscience* 1993;56:241-246.
20. Nilsson P, Laursen H, Hillered L, Hansen AJ. Calcium movements in traumatic brain injury: the role of glutamate receptor-operated ion channels. *J Cereb Blood Flow Metab* 1996;16:262-270.
21. Williams LR, Pregenzer JF, Oostveen JA. Induction of cobalt accumulation by excitatory amino acids within neurons of the hippocampal slice. *Brain Res* 1992;581:181-189.
22. Jansen HML, Pruijm J, Van der Vliet AM, et al. Visualization of damaged brain tissue after ischemic stroke with cobalt-55 positron emission tomography. *J Nucl Med* 1994;35:456-460.
23. Jansen HML, Paans AMJ, Van der Vliet AM, et al. Cobalt-55 positron emission tomography in ischemic stroke. *Clin Neurol Neurosurg* 1997;99:6-10.
24. Jansen HML, Van der Naalt J, Van Zomeren AH, et al. Cobalt-55 positron emission tomography in traumatic brain injury: a pilot study. *J Neurol Neurosurg Psych* 1996;60:221-223.
25. Jansen HML, Knollema S, Veenma-van der Duin L, et al. Pharmacokinetics and dosimetry of 55- and 57-cobalt chloride. *J Nucl Med* 1996;37:2082-2086.
26. Jansen HML, Willemsen ATM, Sinnige LGF, et al. Cobalt-55 positron emission tomography in relapsing-progressive multiple sclerosis. *J Neurol Sci* 1995;132:139-145.
27. Joosten AAJ, Jansen HML, Piers A, Minderhoud JM, Korf J. Cobalt-57 SPECT in relapsing-progressive multiple sclerosis: a pilot study. *Nucl Med Commun* 1995;16:703-705.
28. Orgogozo JM, Dartigues JF. Methodology of clinical trials in acute cerebral ischemia: survival, functional and neurological outcome measures. *Cerebrovasc Dis* 1991;1(suppl 1):100-111.
29. Jacobs A, Put E, Ingels M, Bossuyt A. Prospective evaluation of technetium-99m-HMPAO SPECT in mild and moderate traumatic brain injury. *J Nucl Med* 1994;35:942-947.
30. Dux E, Oschlies U, Uto A, et al. Serum prevents glutamate mitochondrial calcium accumulation in primary neuronal cultures. *Acta Neuropathol* 1996;92:264-272.
31. Furlan M, Marchal G, Vader F, Derlon J-M, Baron J-C. Spontaneous neurological recovery after stroke and the fate of the ischemic penumbra. *Ann Neurol* 1996;40:216-226.
32. Powers WJ, Grubb RL, Darriet D, Raichle ME. Cerebral blood flow and cerebral metabolic rate of oxygen requirements for cerebral function and viability in humans. *J Cereb Blood Flow Metab* 1985;5:600-608.

Evaluation of Carbon-11-Labeled KF17837: A Potential CNS Adenosine A_{2a} Receptor Ligand

Junko Noguchi, Kiichi Ishiwata, Shin-ichi Wakabayashi, Tadashi Nariai, Seigo Shumiya, Shin-ichi Ishii, Hinako Toyama, Kazutoyo Endo, Fumio Suzuki and Michio Senda

Positron Medical Center and Department of Laboratory Animal Science, Tokyo Metropolitan Institute of Gerontology, Tokyo; Showa College of Pharmaceutical Sciences, Tokyo; Department of Neurosurgery, Tokyo Medical and Dental University, Tokyo; and Pharmaceutical Research Laboratories, Kyowa Hakko Kogyo Company, Shizuoka, Japan

The ^{11}C -labeled KF17837 ([7-methyl- ^{11}C](E)-8-(3,4-dimethoxy-styryl)-1,3-dipropyl-7-methylxanthine) was evaluated as a PET ligand for mapping adenosine A_{2a} receptors in the central nervous system (CNS). **Methods:** The regional brain distribution of [^{11}C]KF17837 and the effect of adenosine antagonists on the distribution were measured in mice by the tissue sampling method. In rats, the regional brain uptake of [^{11}C]KF17837 and the effect of carrier KF17837 was visualized by autoradiography. Imaging of the monkey brain with [^{11}C]KF17837 was performed by PET. **Results:** In mice, a high uptake of [^{11}C]KF17837 was found in the striatum in which A_{2a} receptors were highly enriched. The uptake was decreased by co-injection of carrier KF17837 or a xanthine-type A_{2a} antagonist CSC but not by nonxanthine-type A_{2a} antagonists ZM 241385 or SCH 58261, or an A₁ antagonist KF15372. In the rat brain, [^{11}C]KF17837 was accumulated higher in the striatum than in other brain regions, and the uptake was blocked by co-injection of carrier KF17837. In a monkey PET study, a high striatal uptake of radioactivity was observed. **Conclusion:** Carbon-11-KF17837 binds to

adenosine A_{2a} receptors in the striatum. However, the presence of an unknown but specific binding site for xanthine-type compounds also was suggested in the other brain regions. The results also suggested that the in vivo receptor-binding sites of xanthine-type ligands are slightly different from those of nonxanthine-type A_{2a} antagonists.

Key Words: carbon-11-KF17837; xanthine; adenosine A_{2a} receptor; central nervous system; PET

J Nucl Med 1998; 39:498-503

Adenosine is an endogenous modulator of synaptic functions in the central nervous system (CNS) as well as in the peripheral system. The effect is mediated by two major subtypes of receptors: adenosine A₁ receptors, which exhibit higher affinity to adenosine and inhibit adenylyl cyclase, and A₂ receptors, which exhibit lower affinity to adenosine and stimulate adenylyl cyclase. Recent advances in molecular biology and pharmacology have demonstrated the presence of at least five subtypes, i.e., A₁, A_{2a}, A_{2b}, A₃ and A₄ receptors. They act with guanosine triphosphate-binding proteins and are coupled not only to adenylyl cyclase but also to ion channels and phospholipases.

Received Jan. 3, 1997; revision accepted Jun. 12, 1997.

For correspondence or reprints contact: Kiichi Ishiwata, PhD, Positron Medical Center, Tokyo Metropolitan Institute of Gerontology, 1-1 Naka-cho, Itabashi, Tokyo 173, Japan.